

Continuous Production of $\text{Cu}_2\text{ZnSnS}_4$ Nanocrystals in a Flow Reactor

Alexey Shavel,[‡] Doris Cadavid,[‡] Maria Ibáñez,[†] Alex Carrete,[‡] and Andreu Cabot^{*,†,‡}

[†]Departament Electronica, Universitat de Barcelona, Barcelona 08028, Spain

[‡]Catalonia Institute for Energy Research (IREC), Jardí de les Dones de Negre 1, Planta 2, 08930 Sant Adrià del Besòs, Barcelona, Spain

S Supporting Information

ABSTRACT: A procedure for the continuous production of $\text{Cu}_2\text{ZnSnS}_4$ (CZTS) nanoparticles with controlled composition is presented. CZTS nanoparticles were prepared through the reaction of the metals' amino complexes with elemental sulfur in a continuous-flow reactor at moderate temperatures (300–330 °C). High-resolution transmission electron microscopy and X-ray diffraction analysis showed the nanocrystals to have a crystallographic structure compatible with that of the kesterite. Chemical characterization of the materials showed the presence of the four elements in each individual nanocrystal. Composition control was achieved by adjusting the solution flow rate through the reactor and the proper choice of the nominal precursor concentration within the flowing solution. Single-particle analysis revealed a composition distribution within each sample, which was optimized at the highest synthesis temperatures used.

Copper-based quaternary chalcogenides have recently attracted a great deal of attention as low-cost alternatives to conventional absorber materials in photovoltaics.^{1,2} Among them, $\text{Cu}_2\text{ZnSnS}_4$ (CZTS), which has a 1.45–1.51 eV band gap and a high optical absorption coefficient ($>10^4 \text{ cm}^{-1}$), is specially suited for this application.¹ Surprisingly, solution-processed CZTS absorber layers have recently provided photovoltaic efficiencies of up to 10%,¹ much higher than those obtained by vacuum-deposition techniques. This unprecedented goal is probably related to better control of the composition and crystal-phase homogeneity obtained in such a complex quaternary material by solution processing techniques in comparison with vacuum-based ones. At the same time, CZTS shows promising thermoelectric properties, with ZT values of up to 0.36 at 700 K.³ In this field, control of the materials composition has also been shown to be fundamental for optimization of its functional properties.³

CZTS layers have previously been prepared by the decomposition of drop-cast solutions of metal salts⁴ or of the constituent binary semiconductors in hydrazine.^{1a} Nevertheless, the preparation of CZTS inks from quaternary CZTS nanoparticles is still the method that potentially can yield layers with superior compositional homogeneity.^{5–7}

The classical colloidal synthesis procedure based on the decomposition of organometallic precursors is well-established and widely used. Variations of this basic procedure allow the preparation of high-quality nanocrystals of a plethora of

different materials.⁸ However, these synthetic routes have usually been developed and optimized for the production of small amounts of material, which are insufficient for most practical applications. This synthetic strategy is also too labor-intensive to provide a sufficient amount of material by multiple small-scale batch production. Moreover, batch-to-batch repetitiveness may also become an unsolvable problem in a potential attempt to produce large amounts of materials by this method. The obvious scale-up procedure derived from classical colloidal synthesis routes is to maintain the synthetic conditions and concentrations optimized for small batches but to increase the total volume of solvent and thus the size of the reaction receptacle to the required production amount. This simple scale-up technique inevitably results in a degradation of the product homogeneity because of the reduced thermal and compositional uniformity of large volumes of solution, especially in the need of a hot injection step.

Maximization of the solution homogeneity, in terms of composition and temperature, is key for producing nanomaterials with highly uniform and well-controlled characteristics. While a proper escalation of the homogenizing and heating mechanisms is indispensable, the heating and mixing volumes used also must be minimized because of the insufficient thermal and mass transport properties of the solvent. Thus, the natural scale-up procedure for obtaining large amounts of high-quality nanomaterials consist of using a very high frequency of identical and automated batch-to-batch events with relatively small volume batches. In the high-frequency limit, this procedure translates into an automated continuous-flow synthesis procedure.

Several groups have developed microfluidic systems for continuous production of nanoparticles. These previous works focused on the degree of control over the nanoparticle properties offered by this technology but ignored its scale-up potential.^{7–11} In spite of all its advantages, very few reports have been devoted to the large-scale synthesis of nanoparticles in macroscopic flow reactors. Among them, the synthesis of silver nanoparticles⁹ and of CdSe¹⁰ and SnTe nanorods¹¹ in stainless steel reactors and in relatively thick polymeric (1/16 in) and silica glass capillaries (0.2–0.5 mm) should be mentioned, though authors referred to this last system as microfluidic.

Here we report a successful continuous production method to obtain relatively large amounts of quaternary chalcogenide

Received: October 20, 2011

Published: January 2, 2012

nanoparticles, in particular CZTS, with controlled composition. The procedure was used for the preparation of grams of this material with controlled composition under open-air conditions.

Figure 1A shows a scheme of the experimental setup used. The precursor solution for the continuous-flow process was

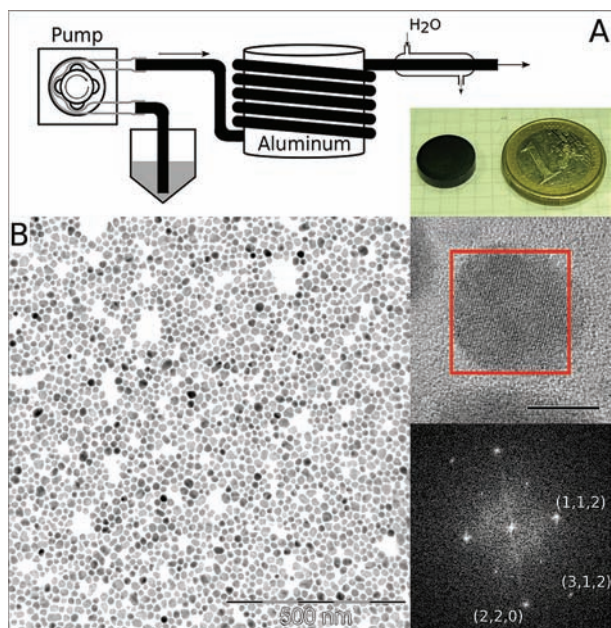


Figure 1. (A) Scheme of the flow reactor setup and image of a 1 g pellet made of CZTS nanoparticles. (B) TEM micrograph of cleaned CZTS nanoparticles prepared inside the flow reactor at 300 °C at a flow rate of 2.0 mL/min. The inset shows an HRTEM image of a CZTS nanocrystal and the corresponding SAED pattern.

prepared by dissolving tin(IV) and copper(II) chlorides and zinc oxide in an oleylamine (OAm, 70%, Aldrich)/octadecene (ODE) mixture. In a typical preparation, 2.0 mmol of $\text{CuCl}_2 \cdot \text{H}_2\text{O}$ (98%, Aldrich) and 1.0 mmol of $\text{SnCl}_4 \cdot 5\text{H}_2\text{O}$ (98%, Aldrich) were initially dissolved in a small amount of tetrahydrofuran (THF) to enhance the solubility of the tin(IV) chloride in OAm. After complete dissolution, 1.0 mmol of ZnO and a certain amount of OAm were added into the solution. The mixture was heated to 50–80 °C in a rotary evaporator. After complete dissolution of the ZnO, the pressure inside the evaporator was reduced to 5–10 mbar to remove THF and any other light products present in the reaction mixture. Just before the synthesis, specific amounts of sulfur and ODE were added to the solution containing the metal complexes. To purify the solution further from any low-boiling-point impurities (e.g., water or light-hydrocarbon impurities from ODE), the mixture was kept at 50 °C and 10 mbar until the sulfur was completely dissolved. The prepared precursor solution was pumped through a 1 m long bronze tube having a 3 mm internal diameter and kept at a temperature in the range 300–320 °C. The flow rate was typically set within the range 1–5 mL/min. The reaction product was collected and washed several times by precipitation with isopropanol and redispersion in chloroform. The final product was readily soluble in various organic solvents (e.g., chloroform, THF, hexane).

A representative transmission electron microscopy (TEM) image of the CZTS nanoparticles produced at 300 °C is shown in Figure 1B. While the nanoparticle size distribution was fairly

narrow, full shape and size control is still not available by this method for such complex quaternary materials. In the inset, a high-resolution TEM (HRTEM) image of a few selected particles and a selected-area electron diffraction (SAED) image of a single nanocrystal are also displayed to show the crystallinity of the obtained products.

The X-ray diffraction (XRD) patterns and Raman spectra of the nanoparticles before and after a sintering treatment at 500 °C (Figure 2) confirmed the crystallographic structure of the

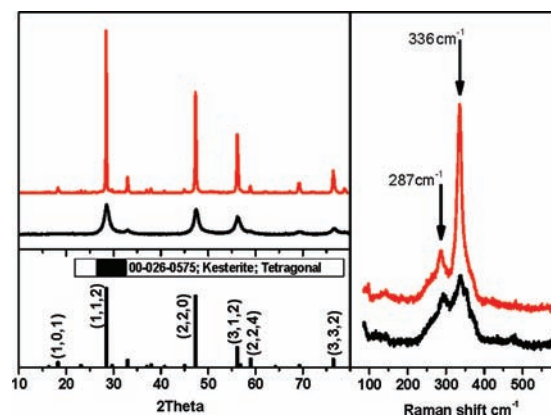


Figure 2. (left) XRD patterns and (right) Raman spectra of the prepared nanoparticles before (black) and after (red) annealing at 500 °C for 1 h. As a reference, the diffraction pattern of $\text{Cu}_2\text{ZnSnS}_4$ (JCPDS no. 00-026-0575) is shown. The lattice parameters for the heated sample were $a = b = 5.40$ Å and $c = 10.40$ Å.

nanocrystals to be compatible with that of CZTS (JCPDS no. 00-026-0575; tetragonal kesterite). CZTS typically crystallizes in a kesterite-type structure (space group $\bar{1}42m$) with two tetrahedral structural units, $[\text{Cu}_2\text{S}]$ and $[\text{SnZnS}_4]$,¹² although CZTS with a wurzite-type crystal structure has recently been reported.¹³ This structure can be derived from zinc blende ZnS by partial substitution of Zn with Cu and Sn.¹⁴ The Raman peaks at 336 and 287 cm^{-1} are the main features of the kesterite-type structure, as previously reported for CZTS.¹⁵

The materials composition was analyzed by scanning electron microscopy–energy-dispersive X-ray spectroscopy (SEM–EDX). For SEM–EDX characterization, the nanoparticles were drop-cast on a silicon substrate. Quite conveniently, the different reaction kinetics of Cu, Zn, and Sn with S allowed us to control the nanoparticle composition over a relatively wide range by appropriately adjusting the precursor concentrations, the reaction temperature, and the flow rate (i.e., the reaction time). Figure 3A shows how the nanoparticles composition depends on the synthesis conditions [see the Supporting Information (SI) for details]. In particular, increasing the flow rate of the solution through the reactor afforded nanoparticles with higher Cu content. From our results, it became evident that the kinetics of the reaction of each element with the sulfur precursor is the fastest for Cu and the slowest for Zn. We believe that initially Cu_2S nanocrystals may nucleate, while first Sn ions and then Zn gradually enter into the nanocrystal structure as the solution advances inside the reaction tube. Lower reaction temperatures extended the time spread needed for the complete incorporation of Zn and Sn ions inside the CZTS crystal structure, thus reducing the possible flow rates available for the formation of stoichiometric nanoparticles.

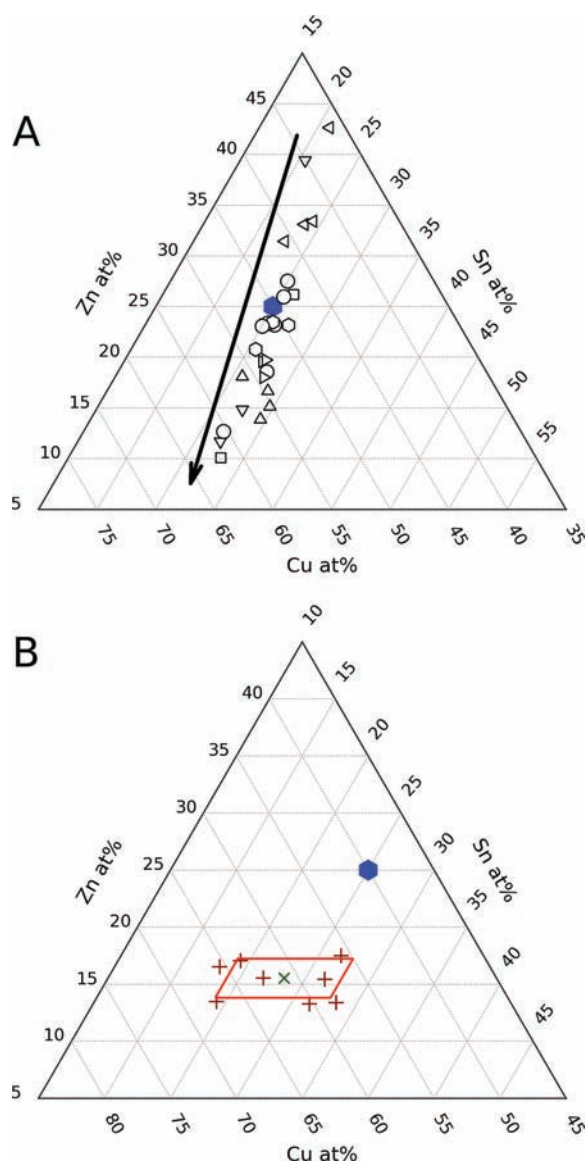


Figure 3. (A) CZTS cationic ratios obtained from SEM–EDX. The arrow points the direction of increasing flow rate. Different symbols denote different reaction conditions (see the SI). (B) Single-particle composition (red +) obtained by HRTEM–EDX analysis of a number of CZTS nanoparticles synthesized at 315 °C. The green × shows the mean composition obtained by averaging the values obtained from several nanoparticles. The blue hexagon in each graph shows the nominal composition of the precursor solution.

It is worth mentioning that although quite a broad range of CZTS compositions were accessible by this procedure, only compositions close to the stoichiometric one were stable after annealing treatments above 500 °C, confirming the narrow stability spot of the CZTS phase.¹⁶ Phase segregation was observed during the annealing treatment for nanoparticles with compositions far from the stoichiometric one (see the SI).

Single-particle HRTEM–EDX analysis confirmed that all of the nanoparticles contained all four elements. However, these analyses also demonstrated the existence of a distribution of nanoparticle compositions within each sample. In this regard, a previous publication demonstrated that while the average composition of a sample of $\text{Cu}_2\text{ZnSnSe}_4$ nanoparticles produced at relatively low temperature (230 °C) by a heating-up procedure was close to the stoichiometric one,

large particle-to-particle compositional variations existed.¹⁷ Figure 3B shows the compositions of several single CZTS nanoparticles prepared at 315 °C. It was experimentally observed that the nanoparticle composition distribution was strongly dependent on the reaction temperature; the lower the reaction temperature, the broader the nanoparticle composition distribution within each sample. As an example, samples prepared at 300 °C showed much larger particle-to-particle compositional differences than those obtained at 315 °C, which showed a fairly good composition homogeneity (see the SI). Notably, no particle with elemental, binary, or ternary composition was found among the several tens of particles checked within each sample.

To measure the thermoelectrical properties of the obtained CZTS nanoparticles, several grams of material were prepared. For these measurements, the CZTS nanoparticles were treated with a formamide solution of $[\text{NH}_4]_2\text{S}$ (20% in water) to remove long-chain organic stabilizers¹⁸ (see the SI for details of the ligand-exchange procedure). The resulting nanoparticles were dried, and the obtained nanopowders were pressed into 13 mm pellets by applying 5 tons of force with a hydraulic press. The materials were then heated to 500 °C in a N_2 atmosphere and maintained at this temperature for 1 h.

The Seebeck coefficient (S) and electrical resistivity of a stoichiometric CZTS sample were characterized over the temperature range 50–350 °C using static direct-current and standard four-probe methods, respectively (Figure 4). Measure-

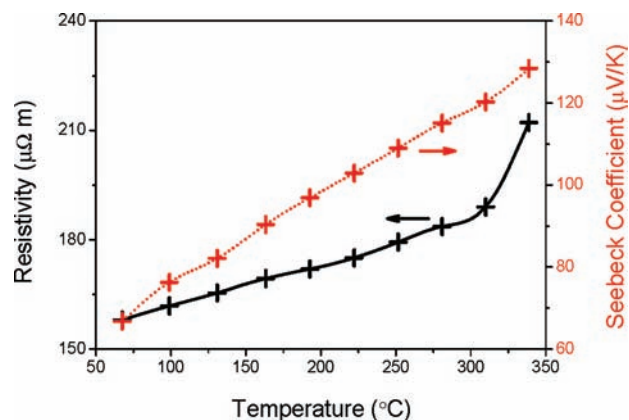


Figure 4. Resistivity and Seebeck coefficient of CZTS nanoparticles pressed into a pellet.

ments were simultaneously carried out under a He atmosphere in an LSR-3 system (LINSEIS). While the Seebeck coefficients obtained for the CZTS nanoparticles were fairly good, the sample resistivity was relatively high. The low electrical conductivities obtained resulted in moderated power factors in the range 0.01–0.1 $\text{mW m}^{-1} \text{K}^{-2}$.

In conclusion, a successful route for the continuous production of $\text{Cu}_2\text{ZnSnS}_4$ (CZTS) nanoparticles has been presented. The preparation procedure allows simple and efficient control of the nanoparticle composition over a wide range. The route was used for the preparation of several grams of CZTS nanoparticles, which were used for the thermoelectric characterization of this material in a nanocrystalline form. Single-particle HRTEM–EDX analysis confirmed the presence of all four elements within each nanocrystal and demonstrated a narrow compositional distribution among nanoparticles within

each sample. The nanoparticle composition distribution was minimized at the highest reaction temperatures used.

■ ASSOCIATED CONTENT

🔗 Supporting Information

XRD pattern of the Sn-rich CZTS sample, distribution of the elements in nanoparticles synthesized at 300 °C, and details of the synthesis parameters used and the ligand-exchange procedure. This material is available free of charge via the Internet at <http://pubs.acs.org>.

■ AUTHOR INFORMATION

Corresponding Author

acabot@irec.cat

■ ACKNOWLEDGMENTS

This work was supported by the Spanish MICINN Projects MAT2008-05779, MAT2008-03400-E/MAT, CDS2009-00050, CSD2009-00013, and ENE2008-03277-E/CON. M.I. thanks the Spanish MICINN for her Ph.D. grant. A.C. is thankful for financial support through the Ramón y Cajal Program.

■ REFERENCES

- (1) (a) Todorov, T. K.; Reuter, K. B.; Mitzi, D. B. *Adv. Mater.* **2010**, *22*, E156. (b) Guo, Q.; Ford, G. M.; Yang, W.-C.; Walker, B. C.; Stach, E. A.; Hillhouse, H. W.; Agrawal, R. *J. Am. Chem. Soc.* **2010**, *132*, 17384. (c) Mitzi, D. B.; Gunawan, O.; Todorov, T. K.; Wang, K.; Guha, S. *Sol. Energy Mater. Sol. Cells* **2011**, *95*, 1421.
- (2) Shavel, A.; Arbiol, J.; Cabot, A. *J. Am. Chem. Soc.* **2010**, *132*, 4514.
- (3) Liu, M.-L.; Chen, I.-W.; Huang, F.-Q.; Chen, L.-D. *Adv. Mater.* **2009**, *21*, 3808.
- (4) Fischereder, A.; Rath, T.; Haas, W.; Amenitsch, H.; Albering, J.; Meischler, D.; Larissegger, S.; Edler, M.; Saf, R.; Hofer, F.; Trimmel, G. *Chem. Mater.* **2010**, *22*, 3399.
- (5) Riha, S. C.; Parkinson, B. A.; Prieto, A. L. *J. Am. Chem. Soc.* **2009**, *131*, 1205.
- (6) Guo, Q.; Hillhouse, H. W.; Agrawal, R. *J. Am. Chem. Soc.* **2009**, *131*, 1167.
- (7) Steinhagen, C.; Panthani, M. G.; Akhavan, V.; Goodfellow, B.; Koo, B.; Korgel, B. A. *J. Am. Chem. Soc.* **2009**, *131*, 12554.
- (8) (a) Ibáñez, M.; Guardia, P.; Shavel, A.; Cadavid, D.; Arbiol, J.; Morante, J. R.; Cabot, A. *J. Phys. Chem. C* **2011**, *115*, 7947. (b) Li, W.; Shavel, A.; Guzman, R.; Rubio-García, J.; Flox, C.; Fan, J.; Cadavid, D.; Ibáñez, M.; Arbiol, J.; Morante, J. R.; Cabot, A. *Chem. Commun.* **2011**, *47*, 10332.
- (9) (a) Lin, X. Z.; Terepka, A. D.; Yang, H. *Nano Lett.* **2004**, *4*, 2227. (b) Huang, J.; Lin, L.; Li, Q.; Sun, D.; Wang, Y.; Lu, Y.; He, N.; Yang, K.; Yang, X.; Wang, H.; Wang, W.; Lin, W. *Ind. Eng. Chem. Res.* **2008**, *47*, 6081.
- (10) (a) Nakamura, H.; Yamaguchi, Y.; Miyazaki, M.; Maeda, H.; Uehara, M.; Mulvaney, P. *Chem. Commun.* **2002**, 2844. (b) Kawa, M.; Morii, H.; Ioku, A.; Saita, S.; Okuyama, K. *J. Nanopart. Res.* **2003**, *5*, 81.
- (11) Jin, H. D.; Chang, C.-H. *J. Mater. Chem.* **2011**, *21*, 12218.
- (12) Liu, M. L.; Huang, F. Q.; Chen, L. D.; Chen, I. W. *Appl. Phys. Lett.* **2009**, *94*, No. 202103.
- (13) Lu, X.; Zhuang, Z.; Peng, Q.; Li, Y. *Chem. Commun.* **2011**, *47*, 3141.
- (14) Chen, S.; Gong, X.; Walsh, A.; Wei, S. *Phys. Rev. B* **2009**, *79*, No. 165211.
- (15) (a) Mitzi, D. B.; Gunawan, O.; Todorov, T. K.; Wang, K.; Guha, S. *Sol. Energy Mater. Sol. Cells* **2011**, *95*, 1421. (b) Shi, L.; Pei, C.; Xu, Y.; Li, Q. *J. Am. Chem. Soc.* **2011**, *133*, 10328.
- (16) Olekseyuk, I. D.; Dudchak, I. V.; Piskach, L. V. *J. Alloys Compd.* **2004**, *368*, 135.
- (17) Haas, W.; Rath, T.; Pein, A.; Rattenberger, J.; Trimmel, G.; Hofer, F. *Chem. Commun.* **2011**, *47*, 2050.
- (18) Nag, A.; Kovalenko, M. V.; Lee, J.-S.; Liu, W.; Spokoyny, B.; Talapin, D. V. *J. Am. Chem. Soc.* **2011**, *133*, 10612.